3-dimensional characterization of thick grating formation in PVA/AA based photopolymer

Sergi Gallego, Manuel Ortuño, Cristian Neipp, Andrés Márquez and Augusto Beléndez

Departamento de Física, Ingeniería de Sistemas y Teoría de la Señal. Universidad de Alicante. Apartado 99, E-03080 Alicante, Spain.
Sergi.Gallego@ua.es

Elena Fernández and Inmaculada Pascual

Departamento Interuniversitario de Óptica. Universidad de Alicante. Apartado 99, E-03080 Alicante, Spain

Abstract: Large thickness is required in holographic recording materials to be used as holographic memories. Photopolymers have proved to be a good alternative to construct holographic memories. Nevertheless, modeling the behavior of thick layers poses some problems due to high absorption of the dye, as discussed in previous papers. In this study, the gratings stored in photopolymers based on polyvinylalcohol/acrylamide (PVA/AA) are analyzed considering the attenuation of light in depth. This is done by fitting the theoretical results, predicted by a model that considers this effect, to the experimental results obtained using diffraction gratings recorded in PVA/AA based photopolymer. In order to determine the diffraction efficiency at the first Bragg angle, an algorithm based on the rigorous coupled wave theory is used. Also, the characteristics of the gratings obtained using different recording intensities are analyzed, and the effective optical thickness is seen to increase as the intensity is increased.

OCIS codes: (090.0090) Holography; (090.2900) Holographic recording materials; (090.7330) Volume holographic gratings

References and links

1. G. Zhao and P. Mouroulis, "Diffusion model of hologram formation in dry photopolymers materials," J. Mod. Opt. **41**, 1929-1939 (1994).
2. J. Lougnot, P. Jost and L. Lavielle, "Polymers for holographic recording: VI. Some Basic ideas for modelling the kinetics of the recording process," Pure and Appl. Opt. **6**, 225-245 (1997).
3. S. Piazzolla and B. K. Jenkins, "First-harmonic diffusion model for holographic grating formation in photopolymers," J. Opt. Soc. Am. B **17**, 1147-1157 (2000).
4. J. T. Sheridan and J. R. Lawrence, "Nonlocal-response diffusion model of holographic recording in photopolymer," J. Opt. Soc. Am. A **17**, 1008-1014 (2000).
5. V. Moreau, Y. Renotte and Y. Lion, "Characterization of DuPont photopolymer: determination of kinetic parameters in a diffusion model," Appl. Opt. **41**, 3427-3435 (2002).
6. R. L. Sutherland, V. P. Tondiglia, L. V. Natarajan and T. J. Bunning, "Phenomenological model of anisotropic volume hologram formation in liquid-crystal-photopolymer mixtures," J. Appl. Phys. **96**, 951-965 (2004).
7. Q. Huang and P. R. Asheley, "Holographyc Bragg gratings input-output couplers for a polymer waveguide at an 850-nm wavelength," Appl. Opt. **36**, 1198-1203 (1997).
8. S. M. Schultz, E. N. Glytsis, and T. K. Gaylord, "Design of high-efficiency volume gratings couplers for line focusing," Appl. Opt. **37**, 2278-2287 (1998).
9. H. J. Zhou, V. Morozov and J. Neff, "Characterization of DuPont photopolymers in infrared light for free-space optical interconnects," Appl. Opt. **34**, 7457-7459 (1995).
10. H. J. Coufal, D. Psaltis and G. T. Sincerbox, eds., *Holographic Data Storage* (Springer-Verlag, New York, 2000).
11. A. Márquez, C. Neipp, A. Beléndez, S. Gallego, M. Ortuño and I. Pascual, "Edge-enhanced imaging with polyvinyl alcohol/acrylamide photopolymer gratings," Opt. Lett. **28**, 1510-1512 (2003).

#68644 - $15.00 USD Received 3 March 2006; revised 16 April 2006; accepted 13 May 2006

12. I. V. Kityk, J. Kasperczyk, B. Sahraoui, M. F. Yasinskii and B. Holan, "Low temperature anomalies in polyvinyl alcohol photoplymers," Polymer **38**, 4803-4806 (1997).
13. A. S. Bablumian and T. Krile, "Multiplexed holograms in thick bacteriorhodopsin films for optical memory/ interconnections," Opt. Eng. **39**, 2964-2974 (2000).
14. D. A. Waldman, C. J. Butler and D. H Raguin, "CROP holographic storage media for optical data storage at grater than 100 bits/μm^2," in *Organic Holographic Materials and Applications*, K. Meerholz, ed., Proc. SPIE **5216**, 10-25 (2003).
15. W. L. Wilson et al., "Realization of high-performance holographic data storage: the InPhase Technologies demonstration platform," in *Organic Holographic Materials and Applications*, K. Meerholz, ed., Proc. SPIE **5216**, 178-179 (2003).
16. S. S. Orlov, W. Philips, E. Bjormson, Y. Takashima, P. Sundaram, L. Hesselink, R. Okas, D. Kwan and R. Snyder, "High-transfer-rate high-capacity holographic disk data-storage system," Appl. Opt. **43**, 4902-4914 (2004).
17. R. R. McLeod, A. J. Daiber, M. E. McDonald, T. L. Robertson, T. S. Slagle, S. L. Sochava and L. Hesselink, "Microholographic multilayer optical disk data storage," Appl. Opt. **44**, 3197-3207 (2005).
18. M. Dubois, X. Shi, C. Erben, L. Longley, E. P. Boden and B. L. Lawrence, "Characterization of microholograms recorded in a thermoplastics medium for three-dimensional optical data storage," Opt. Lett. **30**, 1947-1949 (2005).
19. B. Yao, M. Lei, L. Ren, N. Menke and Y. Wang, "Polarization multiplexed write-once-read-many optical data storage in bacteriorhodopsin films," Opt. Lett. **30**, 3060-3062 (2005).
20. S. R. Guntaka, V. Toal and S. Martin, "Holographically recorded photopolymer diffractive optical element for holographic and electronic speckle-pattern interferometry," Appl. Opt. **41**, 7475-7449 (2002).
21. M. Ortuño, S. Gallego, C. García, C. Neipp, A. Beléndez and I. Pascual, "Optimization of a 1 mm thick PVA/acrylamide recording material to obtain holographic memories: method of preparation and holographic properties," Appl. Phys. B **76**, 851-857 (2003).
22. M. Ortuño, S. Gallego, C. García, C. Neipp and I. Pascual, "Holographic characteristics of a 1 mm thick photopolymer to be used in holographic memories," Appl. Opt. **42**, 7008-7012 (2003).
23. S. Gallego, M. Ortuño, C. Neipp, A. Márquez, A. Beléndez, I. Pascual, J. V. Kelly and J. T. Sheridan, "Physical and effective optical thickness of holographic diffraction gratings recorded in photopolymers," Opt. Express **13** 1939-1950 (2005).
24. S. Gallego, M. Ortuño, C. Neipp, A. Márquez, A. Beléndez, I. Pascual, J. V. Kelly and J. T. Sheridan, "3 Dimensional analysis of holographic photopolymers based memories," Opt. Express **13**, 3543-3554 (2005).
25. J. V. Kelly, F. T. O' Neill, C. Neipp, S. Gallego, M. Ortuño and J. T. Sheridan, "Holographic photopolymer materials: non-local polymerisation driven diffusion under non-ideal kinetic conditions," J. Opt. Soc. Am. B **22**, 407-406 (2005).
26. I. Aubrecht, M. Miller and I. Koudela, "Recording of holographic gratings in photopolymers: theoretical modelling and real-time monitoring of grating growth," J. Mod. Opt. **45**, 1465-1477 (1998).
27. J. V. Kelly, M. R. Gleeson, C. E. Close, F. T. O'Neill, J. T. Sheridan, S. Gallego and C. Neipp, "Temporal analysis of grating formation in photopolymer using the nonlocal polymerization-driven diffusion model," Opt. Express **13**, 6990-7004 (2005).
28. S. Gallego, C. Neipp, M. Ortuño, A. Márquez, A. Beléndez and I. Pascual, "Diffusion based model to predict the conservation of holographic gratings recorded in PVA/Acrylamide photopolymer," Appl. Opt. **42**, 5839-5845 (2003).
29. C. Neipp, J. T. Sheridan, S. Gallego, M. Ortuño, I. Pascual and A. Beléndez, "Effect of a depth attenuated refractive index profile in the angular responses of the efficiency of higher orders in volume gratings recorded in a PVA/Acrylamide photopolymer," Opt. Commun. **233**, 311-322 (2004).
30. C. Neipp, A. Beléndez, S. Gallego, M. Ortuño, I. Pascual and J. T. Sheridan "Angular responses of the first and second diffracted orders in transmission diffraction grating recorded on photopolymer material," Opt. Express **11**, 1835-1843 (2003).
31. M. G. Moharam, E. B. Grann, D. A. Pommet and T. K. Gaylord, "Formulation for stable and efficient implementation of the rigorous coupled-wave analysis of binary gratings," J. Opt. Soc. Am. A **12**, 1068-1076 (1995).

1. Introduction

The parameters that govern the behaviour of photopolymers may be characterised using different diffusion models [1-6]. The parameters obtained depend on the chemical composition used, each chemical composition being optimized for each particular application. Photopolymer applications include grating couplers [7], focusing gratings [8], optical interconnects [9], optical data storage [10], holographic filters [11], acoustooptical deflectors and acoustooptical modulators [12], since these materials have several attractive advantages. In recent years there has been an increase in holographic data storage applications and new companies have developed photopolymer disks for information storage [10, 13-19]. In order to achieve high capacity holographic memories the thickness of the material must be 500 μm

#68644 - $15.00 USD Received 3 March 2006; revised 16 April 2006; accepted 13 May 2006

or more. In this way the material may be competitive with current storage information devices [10]. The high thickness allows us to obtain narrow angular scans and multiple holograms can be recorded overlapped at each location by using hologram-multiplexing methods such as angle, wavelength, phase-code, fractal, peristrophic, and shift multiplexing [10]. In order to optimize the absorbent photopolymers for data storage, low concentrations of dye and monomer are needed to obtain low noise (scattered light) and large values of effective optical thickness. However, in order to obtain high values of dynamic range (*M*#) we need to record many holograms in the same volume with high concentrations of dye and monomer [10]. Therefore, the optimum balance between these characteristics must be found. Nevertheless it is interesting to remark that multiplexing methods can be used to record many diffractive elements in the same volume [20], for example lenses with different focal lengths, applications that are very interesting for many displays.

Using polyvinylalcohol/acrylamide (PVA/AA) based photopolymer it is easy to obtain layers with a physical thickness of around 1 mm [21-22]. The composition of this type of layers has been optimized to record holographic gratings. When modeling the behaviour of these layers using conventional models, thick layers present two important drawbacks. In the first place, the difference between the effective optical thickness and the physical thickness in the material due to the absorption of light inside the material [23], and in the second, the growth of scattered for long recording exposures [21], usually higher than 150 mJ/cm^2. To solve the first problem 3-D analysis has been proposed by our research group taking into account the variation in the absorption of light in the material versus exposure time [24]. In this paper we use this analysis to describe the behaviour of the material in real time and to study different exposure intensities both theoretically and experimentally.

2. Theoretical model

Let us now reintroduce the model used to analyze the grating formation [24]. We propose the use of the following two equations to describe 3-dimensional polymerization

$$\frac{\partial [M](x,z,t)}{\partial t} = \frac{\partial}{\partial x} D(t) \frac{\partial [M](x,z,t)}{\partial x} - k_R(t) I^{\gamma}(x,z,t)[M](x,z,t) + \frac{\partial}{\partial z} D(t) \frac{\partial [M](x,z,t)}{\partial z} \tag{1}$$

$$\frac{\partial [P](x,z,t)}{\partial t} = k_R(t) I^{\gamma}(x,z,t)[M](x,z,t) \tag{2}$$

where n is the refractive index, [M] the monomer concentration, [P] the polymer concentration, D is the difusivity, γ indicates the relationship between the intensity and the polymerization rate, k_R, and $I(x,z,t)$ is the recording intensity attenuated by the dye inside the material, as defined in previous studies [24]

$$I(x,z,t) = I_0 \left[1 + \cos\left(\frac{2\pi x}{\Lambda} \right) \right] \exp[-\alpha(t) z] \tag{3}$$

where I_0 is the average intensity, Λ is the grating period (0.88 μm in this work), and α is the coefficient of the light attenuation.

The absorption of light inside the material as a function of time can be described in a first approximation as follows

$$\alpha(t) = \alpha_0 \exp(-K_{\alpha} I_0^{\beta} t) \tag{4}$$

The initial value of α ($\alpha(0) = \alpha_0$) can be obtained if the transmittance and the physical thickness of the layer are known. In our material for layers with a physical thickness of around 900 μm the transmittance is around 0.5%. In others words, the values of α_0 for this composition are around 0.006 μm^{-1} [24]. β is a constant that determines the influence on the intensity as the dye is consumed and depends on many factors (chemical composition of the

#68644 - $15.00 USD Received 3 March 2006; revised 16 April 2006; accepted 13 May 2006

material, temperature, humidity, etc.). The absorption decay depends on the dye and the intensity used, and K_α defines the rate at which the dye is consumed. In this paper we use β = 0.5 and K_α = 0.005 cm^2 m W^{-1} s^{-1} in our fittings [24].

The Trommsdorff effect describes the evolution of the polymerization rate with time in three steps, firstly the induction period, secondly the autoacceleration, and in the last place the polymerization decreases due to the limitation of the diffusion [25]. We assume that the two first processes are very fast, so we only take into account the decrease in the polymerization rate due to the Trommsdorff effect after the process is initiated. It is given by

$$k_R(t) = k_R \exp(-\varphi {I_0}^{\gamma} t) \tag{5}$$

where φ is the attenuation coefficient of the polymerization rate.

The diffusivity is limited by the presence of polymer, then

$$D(t) = D_0 \exp(-\varphi {I_0}^{\gamma} t) \tag{6}$$

If the thickness of the material is around 1 mm and the period of the grating recorded is lower than 1 μm, then we can assume that

$$\frac{\partial [M](x,z,t)}{\partial x} >> \frac{\partial [M](x,z,t)}{\partial z} \tag{7}$$

Using this approximation the monomer diffusion along the *z* axis can be disregarded, and eqs. (3) and (4) can be solved in a similar manner to that used for the 2-D case.

Our simple approach to solve these equations in order to obtain qualitative information about the behaviour of the material in depth is as follows: The photopolymer film is divided into *G* different sub-films each of thickness d_g; the total thickness of the photopolymer, *d*, is given by the sum of the thicknesses of the different sub-films

$$d = \sum_{g=1}^{G} d_g \tag{8}$$

where *G* is the number of sub-films used. Then we can obtain the Fourier refractive index expansion for each sub-grating.

The refractive index modulation, $n_1(t)$, depends on the refractive indexes of the different components and following Aubrecht et *al*. [26], —with a minor typographical correction (6 appears in the denominator of the first part of the right hand side of the eq. (9) instead of 3 as has been shown in previous papers [24, 27, 28])—, the refractive index modulation can be written as follows

$$n_1 = \frac{(n_{dark}^2 + 2)^2}{6 n_{dark}} \left[-\left(\frac{n_m^2 - 1}{n_m^2 + 2} - \frac{n_b^2 - 1}{n_b^2 + 2} \right) [M]_1 + \left(\frac{n_p^2 - 1}{n_p^2 + 2} - \frac{n_b^2 - 1}{n_b^2 + 2} \right) [P]_1 \right] \tag{9}$$

where n_p is the polymer refractive index, n_m is the monomer refractive index, n_b is the binder refractive index and n_{dark} is the refractive index of the layer before exposure.

In the material used in this study the different refractive indexes take the following values n_m = 1.486, n_b = 1.474 and n_{dark} = 1.478. These values were obtained using the Lorentz-Lorenz equation and the method used is described in references 24 and 26. The calculations are based on refractometer measurements using water solutions.

One of the problems involved in working theoretically with thick layers (where the refractive index profile is attenuated in depth) is calculating the diffraction efficiency around the Bragg angle. It is common in holography to express the profile recorded in the grating in

#68644 - $15.00 USD Received 3 March 2006; revised 16 April 2006; accepted 13 May 2006

terms of the refractive index. For this study we assume that a refractive index profile stored in the sub-layer g, $n_g(z)$, has the form [29-30]

$$n_g(z) = n_{g0} + n_{g1}(z)\cos(Kx) + n_{g2}(z)\cos(2Kx) + n_{g3}(z)\cos(3Kx) \qquad (10)$$

where $K = 2\pi/\Lambda$. In our material $n_3 \leq n_1/8$ and n_3 can be neglected [23, 24]. Therefore they do not affect the values of the higher harmonics in the diffraction efficiency around the first Bragg angle. In this paper we obtain the refractive index profile in each sub-layer using the diffusion model and then we relate the harmonic components of the refractive index to the Fourier components of the dielectric permittivity (ε), provided that $n_1 << n_0$, in order to calculate an algorithm based on Rigorous Coupled Wave analysis (RCW) proposed by Moharam and Gaylord [31]. In this case

$$\varepsilon_{\pm i} = n_0 n_i \qquad \text{for i = 1, 2, 3} \qquad (11)$$

where $\varepsilon_{\pm i}$ are the harmonics of the Fourier expansion of the dielectric permittivity. The method used in this paper is described partially in previous papers [23, 29], but now we don't assume exponential the attenuation of the index in depth. In this paper the values of the refractive index profile are given by the model in each sub-grating. To apply the boundary conditions we assume as in previous papers that there are no reflected orders between the sub-layers inside the material.

3. Experimental

The photopolymerizable solution was prepared, as in previous papers [21, 22], adding yellowish eosin (the dye, 9.00×10^{-5} M), together with a solution of acrylamide (the monomer, 0.34 M) and triethanolamine (the co-initiator, 0.15 M) to a PVA solution (the binder, 13.30% weight/volume). In this study the solutions were prepared using a conventional magnetic stirrer, under red light and in standard laboratory conditions (temperature, pressure, relative humidity). If the viscosity is too high to use a magnetic stirrer, we stir the solution slowly by hand to prevent the formation of air bubbles and then apply a vacuum atmosphere to both the prepared solution and the coated molds so that any eventual air bubbles are completely eliminated [20]. The solutions are deposited, by gravity, in polystyrene circular molds and left in the dark to allow the water to evaporate, while recording in laboratory conditions (temperature and relative humidity) during the process. When a high percentage of the water content has evaporated (around 88%) [20], the "dry" material is removed from the mold, cut into squares and deposited, without the need of adhesive, onto the surface of glass plates measuring 6.5 × 6.5 cm^2. The plates are then ready for exposure, which takes place immediately. On each plate we record four gratings with a spatial frequency of 1125 lines/mm and diameter of 1.5 cm, the experimental set-up used to recorded non-slanted gratings can be seen in previous works [20, 28].

4. Results and discussion

4.1 Behaviour of thick layers in real time

We now present and discuss the fittings of the experimental data taking into account the attenuation of light inside the material. In Fig. 1 we present the fitting of a layer with a physical thickness of around 900 μm and initial transmittance of 0.5% (white dots) for the recording wavelength (514 nm). These data can be obtained before the recording processes using a spectrometer and a conventional micrometer. The grating was recorded using an incident intensity of 6 mW/cm^2. The parameters obtained with the fitting are $D = 2 \times 10^{-10}$ cm^2/s, $k_R = 0.018$ cm $mW^{-1/2}$ s^{-1}, $n_p = 1.506$ and $\varphi = 0.005$ $cm^2 mW^{-1} \mu m^{-1}$. We can see in Figure 1 that with this model the behaviour of the 800 μm and 1000 μm layers is similar during the first 15 seconds. This occurs because no grating is recorded at a depth of over 700 μm inside the layer. We applied the model to simulate different cases of physical thickness using the same parameters (diffusivity, polymerization rate, etc.). We believe it is interesting to note the

#68644 - $15.00 USD Received 3 March 2006; revised 16 April 2006; accepted 13 May 2006

similar behaviour of the layers with a thickness of over 600 µm. This effect is due to the limitation of the optical thickness by Beer's law and to the fact that in last sub-layers of the material no gratings are recorded. This phenomenon cannot be predicted using 1-dimensional models. In these models if higher thickness are studied the grating strengths are higher too [24], and to fit one layer correctly it is necessary to determine the effective optical thickness beforehand. In other words you need to fit the angular response first [23]. For this value of absorption, the results using a 1-dimensional model and the model used in this work are similar only when the thickness of the layer is less than 500 µm.

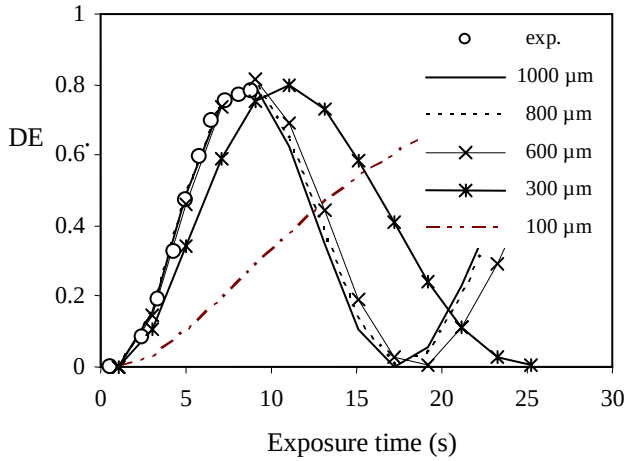

Fig. 1. Diffraction efficiency (DE) versus exposure time for one grating with a physical thickness of 900 µm, the experimental data (white dots) and the simulations using the theoretical model for different thicknesses (1000 µm, 800 µm, 600 µm, 300 µm and 100 µm).

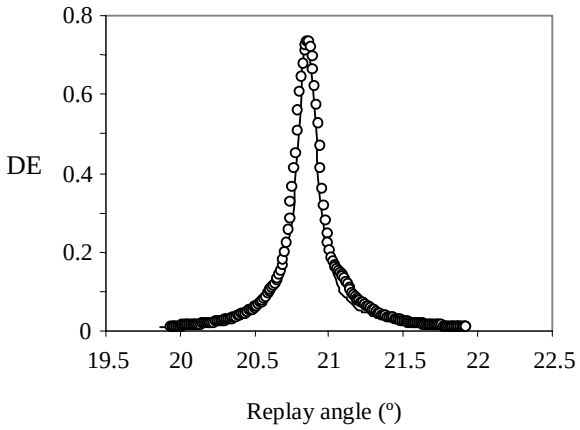

Fig. 2. Diffraction efficiency (DE) as a function of replay angle for the grating presented in Figure 1 (900 µm of physical thickness and spatial frequency of 1125 lines/mm). Experimental (o), algorithm using diffusion model (—).

When we take into account the values of refractive index obtained in each sub-layer using the model to calculate the diffraction efficiency with an algorithm based on RCW, we can see the smoothing of the secondary lobes in the angular scan due to attenuation of the refractive index modulation in depth [23, 29] (Fig. 1). We can see in Fig. 2 how the diffusion model presented predicts the smoothing of the angular response and diffraction efficiency of the

#68644 - $15.00 USD Received 3 March 2006; revised 16 April 2006; accepted 13 May 2006

thick layers. In this case the effective optical thickness [23] of the layer is 690 ± 20 μm and the initial value of the refractive index modulation is 3.10×10^{-4}.

4.2 Gratings recorded with different recording intensities

The predictions of the model were evaluated for different values of recording intensity. The results obtained for 2 mW/cm^2 and 20 mW/cm^2 are presented in Fig. 3. For these intensities we need to expose the layer for around 60 and 5 seconds, respectively, to obtain maximum diffraction efficiency at the Bragg angle. We can see that the effective optical thickness is similar for these two intensities plotted in Fig. 3.

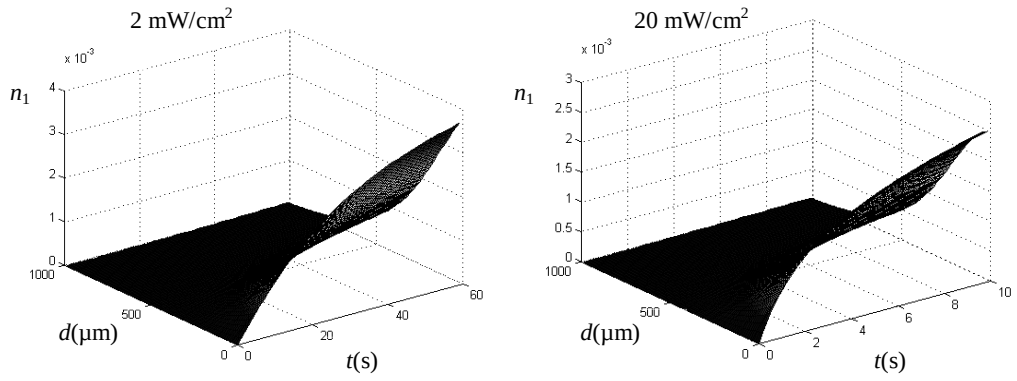

Fig. 3. Refractive index modulation, n_1, as function of the thickness and the exposure time for two different recording intensities: 2 mW/cm^2 and 20 mW/cm^2

Nevertheless, when an experimental analysis is done, differences between the layers recorded using different intensities are observed. In Fig. 4 the angular responses for two different recording intensities, 2 mW/cm^2 and 20 mW/cm^2, respectively, are shown.

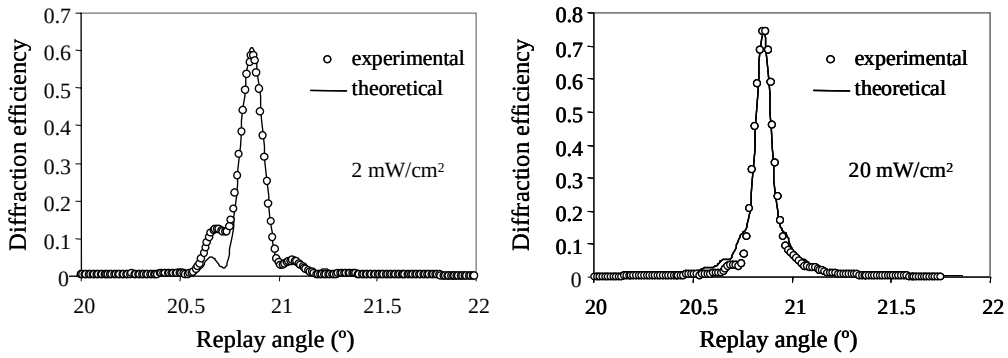

Fig. 4. Angular responses for two different recording intensities: 2 mW/cm^2 and 20 mW/cm^2.

We can see that the central lobe is narrower when higher intensities are used. Then for these high intensities the effective optical thickness of the gratings is greater. In order to fit the experimental data we use the algorithm described in reference 23. We obtain 570 ± 20 μm (intensity of 2 mW/cm^2) and 880 ± 20 μm (intensity of 20 mW/cm^2) as the effective optical thickness of the gratings, and the refractive index modulation near the surface is 3.05×10^{-4} and 4.10×10^{-4}, respectively. The whole study done in the second half of the paper is summarized in Table 1.

#68644 - $15.00 USD Received 3 March 2006; revised 16 April 2006; accepted 13 May 2006

Table 1. Parameters of the gratings recorded using different intensities.

Recording intensity (mW/cm^2)	Exposure time (s)	Effective optical thickness (μm)	Refractive index modulation near the surface ($\times 10^{-4}$)	Maximum diffraction efficiency (%)
2	60	570	4.10	62
6	11	690	3.10	75
20	5	880	3.05	75

The explanation of the differences between the effective optical thicknesses described in Table I can be related to two factors. One is the monomer diffusion in the *z* direction. For low recording intensities we need longer exposures (around 60 seconds) to obtain the maximum diffraction efficiency. Therefore monomer diffusion in the *z* direction plays an important role in grating formation. The other is the low values of recording light in the last sub-layers of the material for small intensities. The layers with a physical thickness of around 900 μm present transmittances of around 0.5% for the recording wavelength. In other words, the recording intensity in the last sub-layer of the material is 10 $\mu W/cm^2$ (whereas the recording intensity in the first sub-layer is 2 mW/cm^2). We checked this effect using similar material and observed that under intensities of 70 $\mu W/cm^2$ no gratings are recorded after 100 mJ/cm^2 of exposure. If an attenuation of light of 0.006 μm^{-1} is considered for a recording intensity of 2 mW/cm^2, then the intensity inside the material at a depth of over 540 μm is lower than 70 $\mu W/cm^2$. Therefore, we believe this to be one of the causes of the small effective optical thickness obtained using an intensity of 2 mW/cm^2. Consequently, the model cannot explain the differences between the optical thickness for different recording intensities and cannot be applied for weak recording intensities. This problem can be solved introducing a recording intensity cutoff value in the model, for intensities lower than this value no gratings can be recorded, this value must be determined experimentally for each dye and photopolymer composition.

5. Conclusions

Good fittings have been obtained using the diffusion model and the algorithm based on RCW for one particular recording intensity. This model permits diffraction efficiency to be fitted as a function of time without previously determining the effective optical thickness of the layer. It is only necessary to know the absorption and physical thickness of the layer. Nevertheless, for large changes in the recording intensities the model has its limitations. The experimental dependence of the effective optical thickness on recording intensity in this type of materials has been shown.

Acknowledgments

This work was supported by the "Ministerio de Educación y Ciencia", Spain, under projects FIS2005-05881-C02-01 and FIS2005-05881-C02-02.

#68644 - $15.00 USD Received 3 March 2006; revised 16 April 2006; accepted 13 May 2006